

**NCHRP 12-68**

**FY 2004**

**Rotational Limits for Elastomeric Bearings**

**Final Report**

*APPENDIX C*

**John F. Stanton**

**Charles W. Roeder**

**Peter Mackenzie-Helnwein**

**Department of Civil and Environmental Engineering**

**University of Washington**

**Seattle, WA 98195-2700**

## TABLE OF CONTENTS

<b>APPENDIX C</b>	<b>TEST APPARATUS AND PROCEDURES</b>	<b>C-1</b>
<b>C.1</b>	<b>Introduction</b>	<b>C-1</b>
<b>C.2</b>	<b>Rotation Tests</b>	<b>C-1</b>
C.2.1	Loading Apparatus	C-1
C.2.2	Control and Instrumentation	C-4
C.2.3	Test Rig Upgrades	C-5
C.2.4	Loading the Rig	C-9
C.2.5	Data Recorded	C-11
C.2.6	Monotonic Tests	C-12
C.2.7	Cyclic Tests	C-12
C.2.8	Procedures for Aspect Ratio, Shape Factor, Material, Shim Edge, and Shear Tests	C-12
C.2.9	Limits on Loading Speed	C-13
<b>C.3</b>	<b>Axial Load Tests</b>	<b>C-15</b>
<b>C.4</b>	<b>Torsion Tests (Diagnostic only)</b>	<b>C-16</b>
<b>C.5</b>	<b>Shear Modulus Test</b>	<b>C-19</b>
<b>C.6</b>	<b>Bulk Modulus Test</b>	<b>C-22</b>

## LIST OF FIGURES

Figure C-1	Multi-Load Bearing Test Rig: Diagram	C-3
Figure C-2	Multi-Load Bearing Test Rig: Photo	C-3
Figure C-3	Multi-Load Bearing Test Rig: Photo of Bearing and Load Cell Detail	C-4
Figure C-4	Leveling Bolt Improvements, Lowered Position	C-5
Figure C-5	Level Bolt Improvements: Raised Position	C-6
Figure C-6	Bearing Support Plate Improvements	C-7
Figure C-7	Ram Support Improvements	C-7
Figure C-8	Ram Swivels	C-8
Figure C-10	Depth Gauge Shown Measuring Bulge	C-11
Figure C-11	Trial Bearing after Testing at Excessive Frequency and Rotation Amplitude	C-14
Figure C-12	Relationship between Temperature Rise and Cyclic Frequency	C-14
Figure C-13	Axial Test Setup Photo	C-15
Figure C-14	$K_T$ ratio vs. $d/L$	C-17
Figure C-15	Torsion box setup	C-18
Figure C-16	Torsion Box with Bearing under Load	C-19
Figure C-17	Steps in Preparation of Shear Modulus Test Specimens	C-20
Figure C-18	Shear test specimen in various stages of production. The knife for peeling off rubber is also shown far right	C-21

Figure C-19	Shear Modulus Test.....	C-21
Figure C-20	Bulk Modulus Test Rig and Sample.....	C-23

**LIST OF TABLES**



## **APPENDIX C    Test Apparatus and Procedures**

### **C.1            *Introduction***

This Appendix describes the test apparatuses and the procedures used during the research. Most of the testing was conducted in the University of Washington's multi-load rig, which can apply static compression, static shear and cyclic rotation simultaneously to a bearing. This rig is described in detail in section C.2. Axial load tests on complete bearings are described in Section C.3, and torsion tests, also on complete bearings, are described in Section C.3. The torsion tests were intended as diagnostic tests to obtain an objective determination of the level of damage incurred by the rotation tests. The torsion tests did not deliver the accuracy needed to be useful and were eventually abandoned, but they are discussed here nonetheless in the interests of completeness. Materials tests were also conducted, on samples cut from the bearings supplied. The shear modulus tests and bulk modulus tests are described in Sections C.4 and C.5 respectively. The tests themselves are relatively standard, but they had to be adapted slightly to allow the use of samples cut from the bearing, rather than specially molded.

### **C.2            *Rotation Tests***

Most tests within this research were conducted on the Multi-Load Bearing Test Rig in the Structures Lab of the University of Washington's Department of Civil and Environmental Engineering. This rig is specifically designed to apply independently-controlled axial loads, shear displacements and rotations to a bearing. The axial load and shear remain constant during a test, but the rotation is controlled by a servo-controlled actuator, which permits the imposition of cyclic rotations, a feature essential to the execution of the tests in this research.

A brief description of the test rig is given in Section C2.1. For more detailed information see Rogers (1989). Subsequent sections describe the procedures used to conduct the various tests in this rig.

#### **C.2.1        *Loading Apparatus***

The rig is shown schematically in Figure C-1, and the photos in Figure C-2 and Figure C-3 show details. It consists of a series of moving parts and a fixed frame against which they react. The fixed frame is made from two ends and a top and a bottom rail, each of which is made from two heavy steel I-beams or channels. The main moving parts are two lever arms, with large load cells attached, that encompass the bearing. (Each lever arm is in fact made from two I-beams, connected together at the top). On the back of each lever arm is a cylindrically curved plate. A set of four 100 ton rams reacts against the loaded end of the fixed frame and compresses the lever arms and the bearing between them. Each curved plate is contact with a thick plate that is supported vertically, so, once the axial load is applied, the weight of the lever arms and bearing can be supported by

friction at the interface between the curved plates and the thick flat plates in contact with them.

The lever arms are connected at their top ends by a 55 kip capacity, servo-controlled, MTS actuator. As it moves in and out, the lever arms roll on the curved plates and rotation is imposed on the bearing. The surface of the curved plates is 51" in diameter. If the lever arms are located relative to one another so that distance between the two rolling surfaces is 51", the rolling occurs without any extension or shortening of the axial load system. If the bearing were a perfect pin, there would be no change in the axial load as the system rotated. To achieve the correct spacing of the lever arms, packing plates are used on either side of the test bearing.

In the absence of additional constraints, this arrangement allows the two lever arms to rotate in the same direction (e.g. both counter-clockwise), even if the MTS actuator is locked. This is clearly undesirable, so diagonal bracing is used to prevent such motion. The diagonal rods have articulated ends, since the angle between them and the lever arms changes as the rig applies rotation to the bearing. Fortunately, provided that the rods are symmetric and cross at the axis of rotation of the bearing, they do not change length during the motion. To maintain zero shear displacement on the bearing, the rods are tensioned equally by manually operated, 20 kip rams, which are locked off hydraulically once the desired rod tension is reached. If some shear force is required in the test, the rods can be tensioned to different loads. Because the axial stiffness of the rods is typically much greater than the shear stiffness of the bearing, the diagonal rods apply something closer to a fixed shear displacement than a fixed shear force.

The maximum moment that can be applied is approximately 2750 in-kips, and is limited by the capacity of the MTS actuator. Its stroke also limits the bearing rotation to +/- 0.08 radians. The maximum axial force that can be applied is 800 kips, although the load is usually kept below this level to avoid fatigue in the fixed frame and the rolling surfaces. The shear force that can be applied may be limited by several considerations. The diagonal bars (5/8" diameter Dywidag) can apply a shear force of approximately 55 kips on the bearing if one pair is tensioned to yield, and the other has almost no tension. However, a shear force this large causes significant friction force, and some slip, at the rolling surfaces. If the test is cyclic, the slip builds up with cycling, and the test must frequently be stopped and all the components re-aligned. The shear force that can be carried without risk of such slip is about 20 kips.

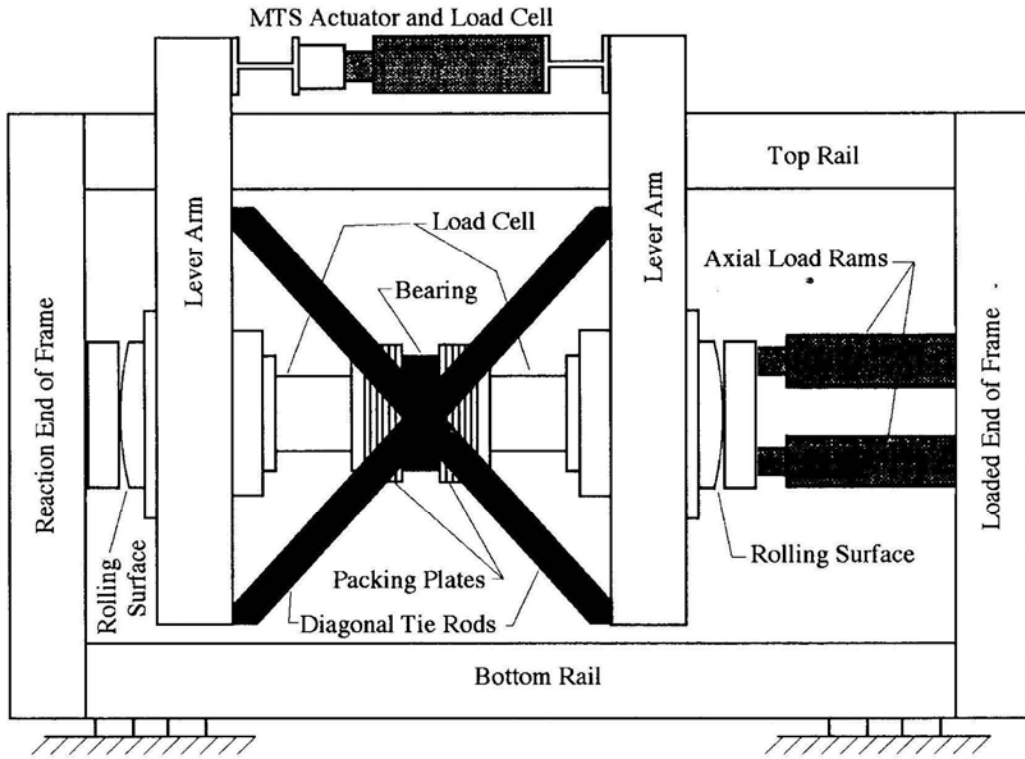


**Figure C-1 Multi-Load Bearing Test Rig: Diagram.**

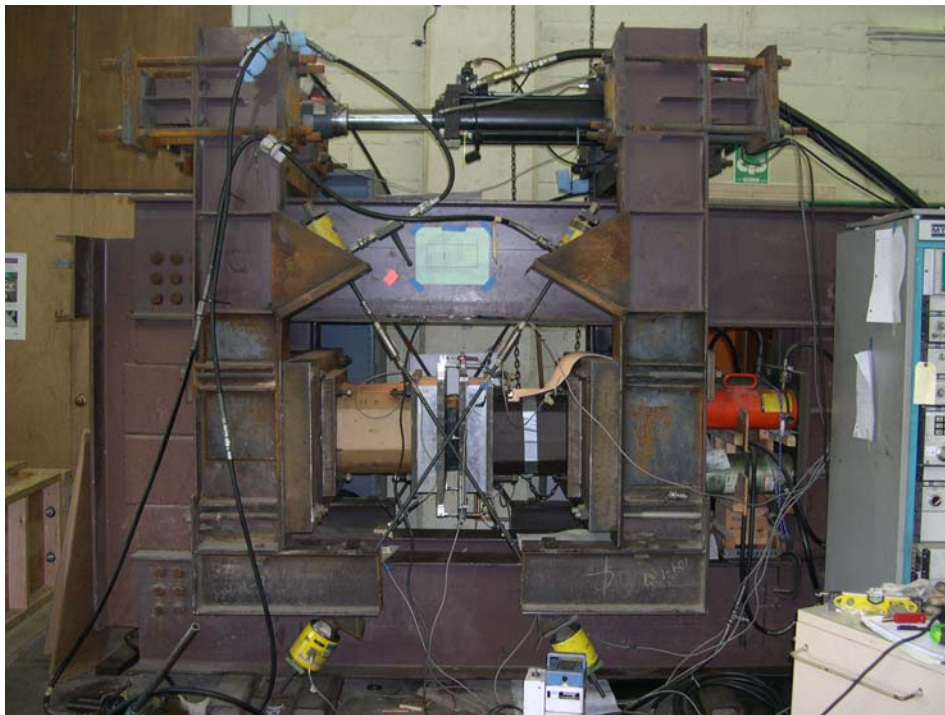


**Figure C-2 Multi-Load Bearing Test Rig: Photo**



**Figure C-3 Multi-Load Bearing Test Rig: Photo of Bearing and Load Cell Detail**

## **C.2.2 Control and Instrumentation**

The axial rams are all connected hydraulically in parallel to a single electric pump, which creates identical internal pressures, and thus equal forces, in each one. The pump is controlled by a manually operated remote control switch. For later tests, an automatic sensor was installed to regulate the axial load; it is discussed in Section C.2.3. The diagonal rods, or shear bars, are controlled by manually-controlled hydraulic pumps.

The servo-controlled MTS actuator that imposes the rotation is linked to an automatic function generator. It can be used to impose a single cycle of rotation, as was the case in the “monotonic” tests, or it can impose many cycles. For the single cycles, a ramp function was used, because the velocity is then constant, and any visco-elastic effects are minimized. During the cyclic tests, a sinusoidal waveform was used because, at the reversal point, a triangular ramp waveform induces an impact that might cause an accumulation of damage to the equipment.

The instrumentation used to record data consists of LVDTs and load cells. Four LVDTs are attached via swivels to the innermost packing plates, adjacent to the bearing, to record the relative displacements of the plates. Two are positioned on the top and two on the bottom so that rotation of the bearing can be derived from the difference. Another LVDT is built into the MTS actuator as well. A load cell in series with the MTS actuator measures the eccentric force that causes the moment on the bearing. The axial force on the bearing is measured by two 800 kip capacity load cells (two were used for



redundancy), and each of the four diagonal rods is equipped with a separate load cell. All of this instrumentation is connected to a National Instruments data acquisition system running LabVIEW software.

### **C.2.3 Test Rig Upgrades**

In its original form, the test rig contained no special devices for aligning the bearing or the moving parts of the rig. Thus the apparatus could be used to run rotation tests, but mounting and aligning a bearing was difficult and time-consuming. Therefore several upgrades were introduced to simplify that process. Some, such as the alignment aids, were built at the start of the research program, while others, such as the diagonal compression struts for the high shear, were only built at the end, when they were first needed. The upgrades are described in this section.

Due to the “floating” design, in which the friction due to axial load is responsible for holding up the lever arms, it is necessary to have an apparatus to support the lever arms when the axial load is not in place. At the top of each lever arm, there are two threaded holes with 1-inch diameter bolts turned down through them.



**Figure C-4 Leveling Bolt Improvements, Lowered Position**

The ends of these bolts rested on the top rail, providing both the needed support and some vertical adjustment. However, the lever arms were still free to move in any horizontal direction during adjustment, which made alignment difficult. A system was therefore constructed to restrict lateral movement to the direction of the axial load.

After careful measurements to determine the centerlines of the reaction frame and both lever arms, slotted steel guide-plates were welded to the top rail, as shown in Figure C-4

and Figure C-5. A brass knob was fixed to the end of each leveling bolt, resulting in a system that allows the movements required for mounting a bearing and for adjustments when the bolts are down (Figure C-4) and allows free movement when they are up (Figure C-5), during testing.



**Figure C-5 Level Bolt Improvements: Raised Position**

The second improvement was made to facilitate mounting the bearing in the rig and to address the problem of the bearing slipping against the packing plates, which tended to occur at rotations larger than about 0.06 radians,. This behavior does not indicate that bearings in the field would slide under the same rotation, because the coefficient of friction between rubber and smooth steel, especially under cyclic conditions, is very different to that between rubber and relatively rough concrete or grout.

Four steel flat bars were welded, one at the top and one at the bottom, to each of the two innermost packing plates, as shown in Figure C-6. The goal was to hold the bearing in the proper vertical location throughout the duration of the test. The flat bars are 3/8-inch thick, and thus engage that the outermost steel shim in the bearing. (If the flat bars had been only 1/8" thick, they would have engaged only the rubber cover on the bearing, and they would have been ineffective in preventing slip). The flat bars are approximately 23 inches long so that the entire length of the 22-inch dimension of the bearing is restrained. Only three sides of the plate were fillet welded so that the edge in contact with the bearing remains square. These bars serve two purposes: One is to provide a platform on which the bearing rests before the axial load is applied so that it is in the correct position

when loaded. The second is to prevent the bearing from slipping during large-rotation monotonic tests.



**Figure C-6 Bearing Support Plate Improvements**



**Figure C-7 Ram Support Improvements**

The third modification was to make a steel frame to maintain accurate alignment of the axial load rams. The need for this became apparent when one of the rams suffered serious gouging, and had to be replaced, due to its developing slight mis-alignment during the many cycles of testing.

A steel frame, shown in Figure C-7, was constructed to hold the axial rams in place more precisely than the simpler system that had been used before. Holes equal in diameter to the ram outer diameters were cut out of two 1/2-inch thick steel plates. One plate was slid over the front of the rams and the other plate was slid over the back of the rams. The plates were then welded together by angles so that they remain in place.

The fourth modification concerned protection of the axial force rams. Late in the testing, it was noticed that the rotation of the curved plates was causing movements of the pistons in the hydraulic rams perpendicular to the axes of the rams. This caused internal wear and leaking of hydraulic fluid. A system was designed to attach a swivel to the end of each ram by way of a connecting part that slides into the center hole of the ram, shown in Figure C-8.

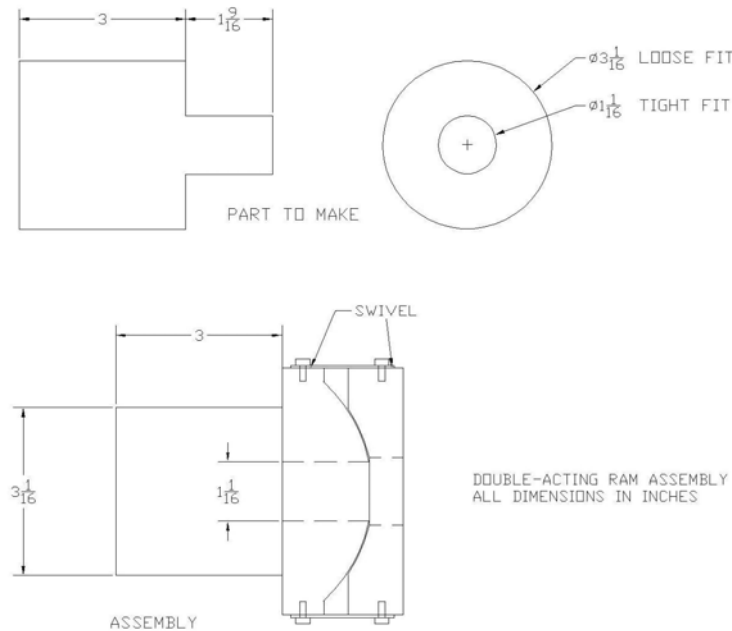


**Figure C-8 Ram Swivels**

The fifth modification was to the diagonal rod system for shear. In the original form of the rig, each rod had a tension-only connection at each end, and the rods were anyway too slender to resist any significant compression. Furthermore, the differential tension system led to shear forces at the rolling surfaces, which could not be resisted without slip by friction. After the first shear test, it was found that the maximum shear displacement that the diagonal tie rods could apply was less than 50%.

A modification was therefore designed by which two of the rods were replaced by compressions struts, which would complement the tension in the two remaining diagonal rods. By using equal and opposite forces in the diagonals, the shear forces at the rolling

interfaces could be eliminated, thereby increasing the shear force and displacement that could be applied to the bearing. The strut is a 2-inch diameter rod with a hole bored into one end. A piston slides through a center-hole jack and into this hole to provide the extension. The ends thread into cylindrical rockers that pin into holes in the plates they bear upon. Two quarter-inch thick plates were replaced with half-inch plates to provide a stronger bearing surface at the bottom of the lever arms. The design of the system was highly constrained, because of the lack of space and because of the need to carry compression in a strut that consisted of several pieces that could not be rigidly welded together. This improvement was used only for the tests where large shear deformations were required.

The sixth and final improvement was the development of a simple servo-control system to maintain the pressure in the axial rams. Due to small leaks in the hydraulic system, especially when the rams were operating near their maximum oil pressure of 10,000 psi, the axial load would drop slightly when the test was left running. A relay switch was therefore connected to the data acquisition system that would be activated when the axial load measurement dropped below a certain level, causing the remote control switch of the pump to be activated. This system ensured that the desired axial load was maintained for the duration of the test.

#### **C.2.4 Loading the Rig**

Each bearing is prepared for its test and loaded into the test rig in a similar fashion. To prepare the bearing, there is only one step. The centerlines of all four side faces are marked with a liquid paper pen. These provide white stripes that contrast with the black rubber of the bearing so that bulge profiles can be more clearly seen when the bearing is tested.

A number of steps must be completed on the rig before the bearing can be loaded. First, the equipment must be turned on. This includes, separately, the data acquisition system, computer, axial ram pump, and MTS system. The MTS system should be zeroed by turning the set point knob until the meter in Figure 9 is in the center so that the actuator does not suddenly shift. Subsequently, the MTS system must be pressurized, first by setting it to “low” and allowing the low pressure to build and then by setting it to “high” and allowing the high pressure to build. Then the MTS actuator is used to rotate the lever arms into a vertical position. It is likely that the lever arms are not at the correct heights so they must be leveled. Leveling was made much simpler by the slotted guide-plates fitted at the start of the test program. The 10-ton overhead crane in the structures lab can be used to raise each lever arm, and each lever arm has a mark to align with the top of the top rail of the reaction frame. With the lever arm raised to this position, the leveling bolts are then lowered into their slots. A magnetic level is attached to the lever arm to ensure that each bolt is extended to the same length, and if not, they are then adjusted accordingly. When the arm is raised and leveled, the crane is detached and the leveling procedure is complete.

With the lever arms in place, the rig is now ready for the bearing to be set in place. The axial rams are pressurized manually so the lever arms move closer together until they are

about three inches apart (for the typical 2.35” thick bearing). The bearing is then lifted by hand into position over the two innermost packing plates and dropped into place, catching one of the welded steel flat bars. For consistency, the bearings are inserted facing the same direction for each test, with the manufacturer’s printed marks facing up and read with the top facing north. The axial rams are then extended until they force the innermost packing plates to touch the faces of the bearing, and then extended a little more to apply a small axial load to the bearing. Then the MTS actuator is used to align the lever arms so that the imposed rotation on the bearing is zero.



**Figure 9 MTS Controls with Set Point Dial in Lower Left and Meter in Upper Right**

The bearing is then pre-conditioned, or “scragged” to remove any crystallization that might have built up in the rubber. The axial load is increased to 200 kips, held for five minutes, and then released to about 30 kips. This is repeated twice more. Once scragging is complete, the axial load is then increased to the correct test load, typically 371 kips or 520 kips, and the MTS actuator is again used to align the packing plates to be parallel, so that the test starts at zero rotation. The nuts at the ends of the four diagonal bars are then hand-tightened so that the rounded plates on which they rotate do not slip and then the diagonal bars are jacked to a load from 1–2 kips. If there is any visible shear deformation in the bearing, it is taken out by applying a further load to the appropriate diagonal bars, typically not to more than a total of 8 kips per bar.

The final step is to install the LVDTs at the innermost packer plates. The outer ends of the LVDT pistons are threaded and screw into corresponding receptacles. The LVDT barrels are gripped in custom-made clamps. Once the LVDTs are fixed to the packing plates, lateral and vertical adjustments are made as necessary to ensure that the axis of the LVDT is horizontal and parallel to the axis of the test rig. Once the LVDTs are installed,

the data acquisition system is re-zeroed, and the leveling bolts are raised. The bearing is now in place, the lever arms are floating freely, and testing can begin.

### **C.2.5 Data Recorded**

Three types of data are recorded. First is the automatic LabVIEW data acquisition system, which records the displacements of the five LVDTs and the loads in the seven load cells to a computer data file. The system can be set to record at a preset time interval (ie. every minute, every hour) or record a certain amount of data given a trigger (ie. if an LVDT displaces one inch, record for ten seconds). Second is the manual measurement of the top and bottom bulge heights using a precision depth gage. This gage is set between two rods that are bolted to the packing plates, as shown in Figure C-10. These rods provide a level reference point from which to measure. Depth gage values are read at the peaks of the bulges of each rubber layer, and are marked so the measurement is taken at the same location throughout the test. The measurement points lie at the middle of the long sides of the bearing, both top and bottom. Third is the recording of cover debonding from the shims by visual and touch methods. When what was previously two bulges from two individual layers becomes one continuous bulge over the two layers, it is considered debonded. The length of debonding on each shim (two top, two bottom) is measured to the nearest inch and recorded. (Measurements could not be taken at the outer two shims, because they were obscured by the steel flat bars that restrained slipping). Photographs of the bearings in various stages of debonding are also taken periodically throughout the test.



**Figure C-10 Depth Gauge Shown Measuring Bulge**

### **C.2.6 Monotonic Tests**

The monotonic tests really consisted of a single cycle of rotation, applied very slowly, in order to minimize any visco-elastic effects. Once the bearing is in place and the axial load is applied as described in Section C.2.4, the first manual recordings are taken. Initial depth gage values are noted, as is debonding, if any. In most cases there was no debonding at the start of the test. After these manual recordings, the MTS system is started and the test rig begins to rotate the bearing, reaching the peak rotation of 0.08 radians in two hours. The test is paused every 1% of rotation and returned to zero to record depth gauge and debonding measurements and take photographs. Any uplift is also noted. After the recording, the rig is returned to its rotated state prior to the pause, and the test is resumed. The pause and return to zero was necessary because the peaks of the bulges were often obscured, at least on the “compression” side of the rotated bearing. After reaching its peak, the rotation is returned to zero over twenty minutes, with no pauses to take readings because no additional damage was expected during the unloading quarter cycle. The exact same procedure is then repeated to 8% rotation in the opposite direction.

### **C.2.7 Cyclic Tests**

The procedures for the cyclic tests are very similar to those for the monotonic rotation tests. The bearing is put in place the axial load is applied, and the initial bulge height readings are taken as before. The desired amplitude and frequency of the rotation are then set on the function generator. Most tests were run at a frequency between 0.2 Hz and 0.5 Hz, and with an amplitude of  $\pm 0.0375$ ,  $\pm 0.025$  or  $\pm 0.0125$  radians.

Initial recordings are made in LabVIEW by manually recording the first two cycles of rotation. After that, LabVIEW is set to automatically record two cycles at regular intervals every 60 to 200 cycles. Tests at  $\pm 0.025$  radians rotation are not expected to debond as soon as those at 0.0375 radians, so the tests run longer and data is recorded less frequently, at every 200 cycles. If, for these longer tests, data were recorded every 60 cycles, the computer would run out of memory before the test was finished and data would be lost.

The bearing is checked periodically throughout the test; there is no regular interval because the tests can run anywhere from six hours to two weeks. If there is new debonding, the MTS system is paused and moved back to zero rotation to record bulge heights. The amount of debonding is also noted and photographs are taken. The MTS system is returned to the rotation at which it was paused, and cyclic loading is resumed. The data acquisition system does not need to be paused explicitly because its action is triggered by the cycle number, and not by time.

### **C.2.8 Procedures for Aspect Ratio, Shape Factor, Material, Shim Edge, and Shear Tests**

The procedure for executing the aspect ratio, shape factor, shim edge and material tests is exactly the same as that for the cyclic tests. Here “Material Test” refers to the rotation test conducted on the non-standard material, not to be confused with the material property



tests. For the aspect ratio and shape factor tests described in Appendix A, only the loads need to be changed.

For the high shear tests, the same steps are also used, but the diagonal compression struts discussed in Section C.2.3 must be installed to apply the required shear force or displacement. This must be done while the axial load is being applied, because the pins on the strut ends need to fit into the mating holes on the lever arms. The struts are quite heavy and both must be installed simultaneously. Once they are in place, the hand jack is used to apply the load as it is for stressing the diagonal tension rods.

### **C.2.9 Limits on Loading Speed**

Elastomeric bearings are not perfectly elastic. During cyclic deformations the bearings dissipate some energy through hysteresis and heat up. Excessive temperature increase causes the cured rubber to break down due to changes in the polymer cross-linking, and therefore changes its physical properties. Changes in the physical properties affect the performance of the elastomeric bearings.

The rotational testing for this project had to be conducted at an accelerated rate in order to accumulate enough cycles on each bearing to cause significant damage within the time available. Therefore it was necessary to determine how fast the tests could be conducted without the risk of excessive heat build-up. A short experimental study was undertaken to find the combinations of rotation amplitude and frequency of the cyclic load that would lead to critical temperature increases. That study is described in this section.

The budget for the project did not allow extra bearings to be ordered for this purpose, so five discarded bearings, donated by Scougal Rubber Company, were used for the study of loading speed. The bearings had been rejected for reasons such as inaccurately placed internal shims, cover flaws, etc., and were, therefore, deemed acceptable for the purpose of establishing approximate thermal response. They were made from neoprene and natural rubber with durometer hardness in the range of 50 - 60 on the Shore A scale, and so represented typical bridge bearings. They had a variety of dimensions.

The bearings were tested at various frequencies and amplitudes of rotation and the internal temperatures were measured with thermocouples drilled in at the mid-point of the long side of the bearing. It was found that the bearing heated up with cycling, but that its temperature approached an asymptotic value, provided that no debonding or other damage occurred. Debonding changed the internal structure of the bearing and, consequently, the rate of energy dissipation and internal heat generation. In one case, with a high frequency and a large rotation amplitude, the bearing essentially melted and suffered major damage. Figure C-11 shows it after testing.

An analytical model was developed to model the heating effects, and the parameters in it were identified from the test results. Details of the testing, analysis and assumptions are given in White (2006).



**Figure C-11 Trial Bearing after Testing at Excessive Frequency and Rotation Amplitude.**

The analytical model was then applied to the standard bearing size (22" x 9") used for the majority of the rotation tests in this research. The predicted relationship between cyclic frequency and the asymptotic temperature rise,  $\Delta T_{inf}$ , is given in Figure C-12 for various rotation amplitudes. That graph was used as a guide for selecting rotation frequencies for the rotation tests described in Appendix C. Thermocouples were not used to verify temperatures in those rotation tests because they require a hole to be drilled at a location that is critical for stress. Drilling the hole might have caused spurious damage. The bearing temperature was monitored approximately by touch instead.

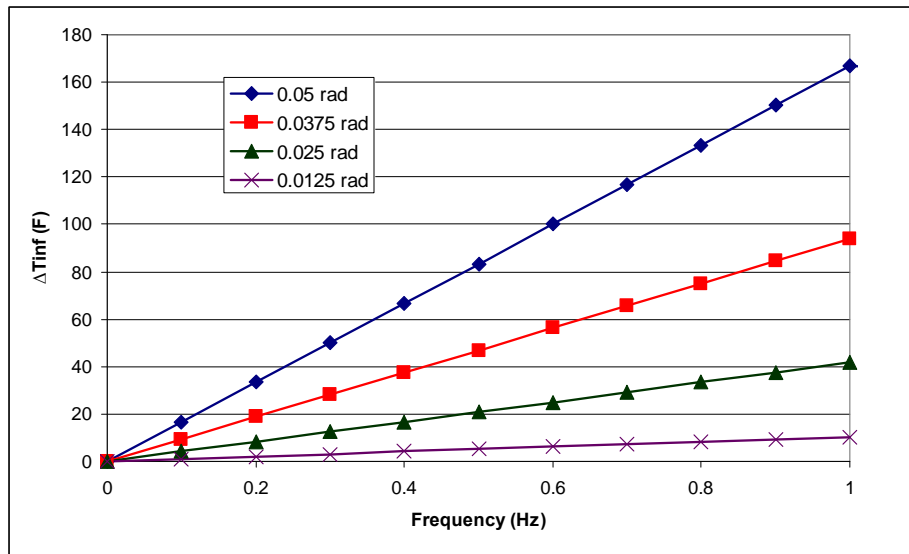


**Figure C-12 Relationship between Temperature Rise and Cyclic Frequency.**

### **C.3 Axial Load Tests**

A minimum of two pure axial tests were performed on each batch of bearings. The test rig used was the 2.4 million pound Baldwin Universal Test Machine in the Civil Engineering Structures Lab at the University of Washington. It was used in preference to the rotation rig because its capacity is higher.

The setup is relatively straightforward and is shown in Figure C-13. The primary need is for a solid reaction plane parallel to the Baldwin's test head. It is also desirable that the plane be raised up slightly from the lower platen, to facilitate observation of the bearing. To achieve it, two steel blocks, each 15 inches by 26 inches in plan area by 8 inches thick, with machined top and bottom surfaces, are stacked on top of thin wooden shims. Then a timber dam is placed around the stack and one 5-gallon bucket of hydrostone is poured into it. It penetrates under the steel plate and around the timber shims.



**Figure C-13 Axial Test Setup Photo**

Before the hydrostone sets, the head of the test machine is lowered onto the upper steel block, and a small load is applied. This load is left in place until the hydrostone sets. When, later, the test head is raised, the steel blocks are solid and parallel to the test head.

To start the test, a bearing with centerline marks is placed on the base and the marks are lined up with the centerlines of the test rig. Then a steel plate is placed on top of the bearing so that the cover rubber does not flow up into the threaded holes in the test head. Two 1-inch potentiometers are hot-glued onto the sides of the base to record displacement as the bearing compresses. These potentiometers, and the load readout from the test machine, are fed into to an HP 4397A data acquisition system running Data Logger software. These data are recorded once each second for the duration of the test.

The two standard tests are the monotonic step load axial test and the cyclic axial test. The only way they differ is in the application of load—the setup is the same. For the

monotonic step test, the test machine head is lowered until it just contacts the bearing and a load registers on the data acquisition system. Initial readings are taken. The load is then raised to 600 psi and held constant for five minutes. It is then raised another 600 psi and held, a process that is repeated until the load reaches at least 6,000 psi. The load can then be lowered back to zero or it can be increased continuously until either the bearing fails or the test machine reaches its 2.4 million pound capacity at about 12,000 psi axial stress on the bearing.

For the cyclic test, the load is raised continuously to 8,000 psi over the course of one minute and then lowered to nearly zero over the course of one minute. This process is repeated until debonding is noted and does not continue to increase. Photographs are taken throughout all tests.

#### **C.4 Torsion Tests (Diagnostic only)**

The torsion tests were designed to serve as objective measures of the extent of debonding, and, by implication, of damage. The results from them did not fulfill the original hopes, and they were therefore abandoned. They are described here nonetheless, in the event that they might be adapted for successful use in future research.

The test was designed to cause torsion about the axis normal to the plane of the shims in the bearing, as shown in Figure C-15. The torque causes shear stress and strain in the rubber. St. Venant Torsion theory shows that the maximum values occur at the mid-points of the two long edges of the bearing. This is exactly where the shear stresses and strains due to compression and rotation are largest, and, therefore, where the most debonding damage would be expected during a rotation test. If such damage were to occur, the torsional stiffness would be expected to change. By testing the bearing in torsion before and after a rotation test, it was hoped that a change in torsional stiffness could be used as an indicator the amount of damage that occurred. For this reason the torsion test appeared to be a simple, objective, yet reasonably sensitive way of measuring damage incurred during rotation.

The sensitivity of the test was estimated as follows. If the bearing is treated as undergoing St. Venant torsion, its torsional stiffness is

$$K_T = \frac{GJ}{T} = \frac{G}{T} c_T L^3 W \quad (C-1)$$

Where

- $T$  = total rubber thickness,
- $L$  = length of short side (usually parallel to the bridge span),
- $W$  = length of long side,
- $c_T$  = coefficient  $\approx 1/3$ .

If debonding occurs along both long sides of the bearing, penetrating to a depth  $d$  on each side, then the effective short dimension becomes  $(W-2d)$ . Ignoring changes in  $c_T$  caused by the slight change in shape leads to

$$K_{T, ratio} = \frac{K_{T, damaged}}{K_{T, undamaged}} = \frac{(L-2d)^3}{L^3} = \left(1 - \frac{2d}{L}\right)^3 \quad (C-2)$$

Figure C-14 shows a plot of the relationship between the  $K_T$  ratio and the penetration ratio ( $d/L$ ). For example, 0.5 inches of debonding along each long side is predicted to lead to a  $d/L$  value of  $0.5/9 = 0.0555$  and a  $K_T$  ratio of 0.70. The implied 30% reduction in torsional stiffness was expected to be detectable quite easily.

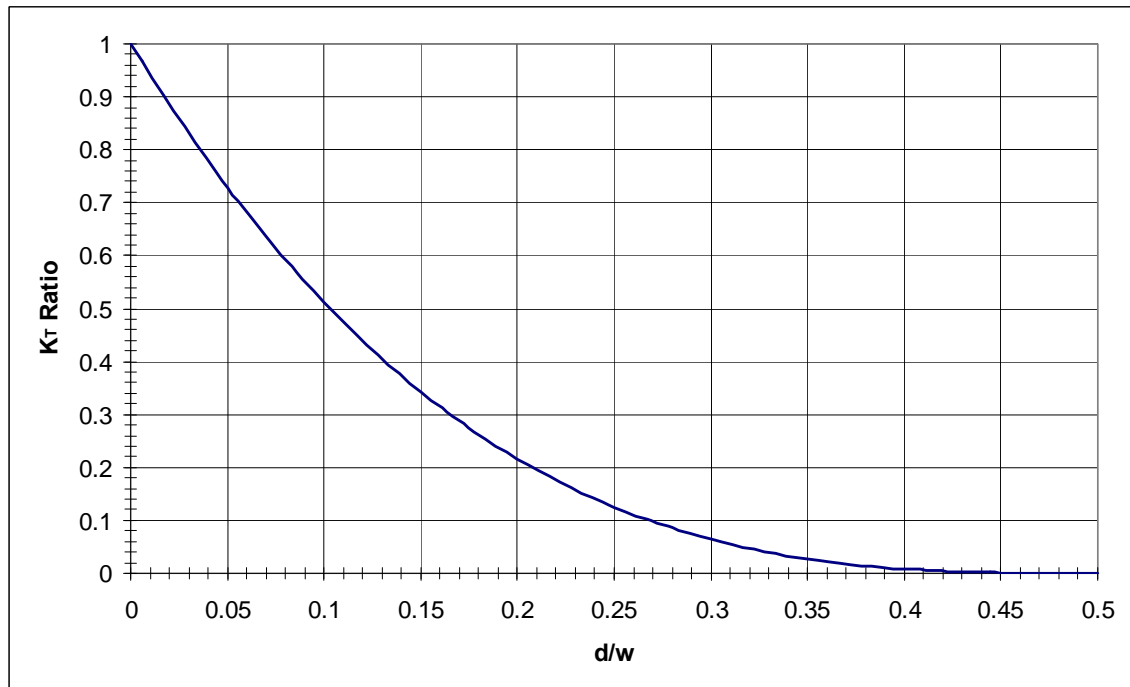


**Figure C-14**  $K_T$  ratio vs.  $d/L$

Figure C-15 and Figure C-16 show the torsion box that was used for the torsional tests. It consists of two vertical metal plates between which the bearing is placed. (Channels were in fact used in place of plates, for reasons of expediency). The bearing is oriented with its shims in the vertical plane and is supported at each face on a sloping steel support member. These two members slope in opposite directions, and contact the outer shims of the bearing to which they provide support. An axial load is applied to the top of the bearing at mid-length of the long edge by placing it on the table of the laboratory's 300-kip Baldwin Test Machine and bringing down the test head to make contact with the load distribution plate on top of the bearing. Because the bearing support reactions are at diagonally opposite corners of the bottom face, the bearing experiences torsional loading.

To reduce friction between the bearing and the inside faces of the torsion box, a greased PTFE sheet was inserted between the channel and the bearing. The two channels were

bolted together to prevent them from being pried apart, and the bearing falling off the sloped supports, during the loading.

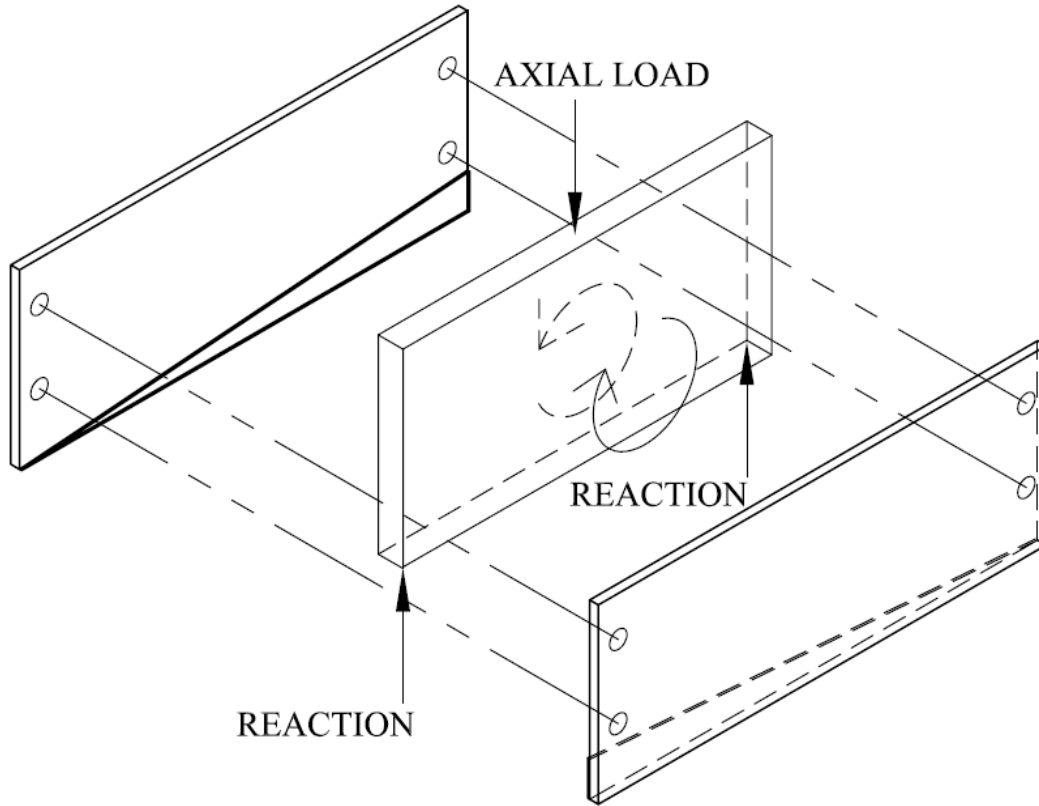


**Figure C-15 Torsion box setup**

Figure C-16 shows a typical bearing under load inside the torsion box. By recording the displacement of the top outer bearing edges opposite the sloping support members, a torque vs. twist angle plot can be obtained.

For each torsional diagnostic test, five cycles are applied to the bearing, but only the last cycle is used for determining the torsional stiffness. This procedure pre-conditions the bearing by eliminating any effects of prior crystallization of the rubber, and is similar to the procedure for the shear modulus test described below.

Torsion test were conducted before and after conducting rotation tests on some of the first bearings. Despite the obvious signs of debonding damage during the rotation test, the torsional stiffness varied so little, and showed significant scatter, that it was unable to predict the likely damage that appeared to be present. An attempt was then made to calibrate the torsion procedure rationally. A new bearing was subjected to torsion testing, and an initial stiffness was obtained. Then a utility knife was used to separate the rubber from the shims, to a known depth of 0.5 inches, all round the bearing. The bearing was then re-tested in the torsion box, but its measured torsional stiffness was found to have changed by less than 2%, whereas Equation (C-2) predicted a 30 % change. The test was thus abandoned.

It is believed that the discrepancy is caused by the fact that the bearing cannot, in fact, be characterized by St Venant Torsion, because significant warping displacements occur. Such displacements were not visible to the naked eye, and the fact that the side channels were bolted together might also be expected to suppress any warping displacements. Despite these facts, warping is considered the most likely reason for the poor results.



**Figure C-16 Torsion Box with Bearing under Load**

## **C.5 Shear Modulus Test**

The shear modulus tests were conducted both to provide input to the Finite Element analyses and to provide a check on the values supplied by the manufacturers for their products.

The shear modulus test is conducted in accordance with the quad shear setup defined in ASTM D4014 but the test specimens are cut from the bearings rather than being specially molded. The test specimens were initially cut to have rubber blocks with dimensions of 2" wide by 5" long. After being tested with these dimensions, the specimens were cut down and tested again, to determine the effect of specimen aspect ratio. The process was repeated three times. In all, four different rubber block lengths (5", 3", 2" and 1.5") were used.

The process for making a test specimen is illustrated diagrammatically in Figure C-17 and photographs of specimens, in various stages of preparation, are shown in Figure

C-18. A 2-inch by 22-inch section is cut with a band saw down the center of a bearing through all the shims and rubber layers. This narrow “sandwich” is then turned on its side and another cut is made down the length of the center rubber layer. The result is two rubber–steel–rubber–steel–rubber “sandwiches” that are each 2 inches by 22 inches by approximately 1.125 inches thick. The two, thin, outer rubber layers of these sandwiches are removed using a custom-made knife to leave two pieces each with clean steel on both faces bonded to a single layer of rubber in between. The band saw is then used to cut through one of the steel layers at the midpoint of the 22-inch dimension. The opposite steel layer is similarly cut 5 inches either side of the midpoint and all three cuts are extended through the rubber layer to the opposite steel layer by using a utility knife. The band saw and custom-made knife are then used to remove the rubber that is not in the 5-inch center sections. The final result is two identical pieces that each have one 22-inch long steel plate cut at the center attached through two half-inch thick 2-inch by 5-inch rubber segments to one continuous 10-inch long steel plate.

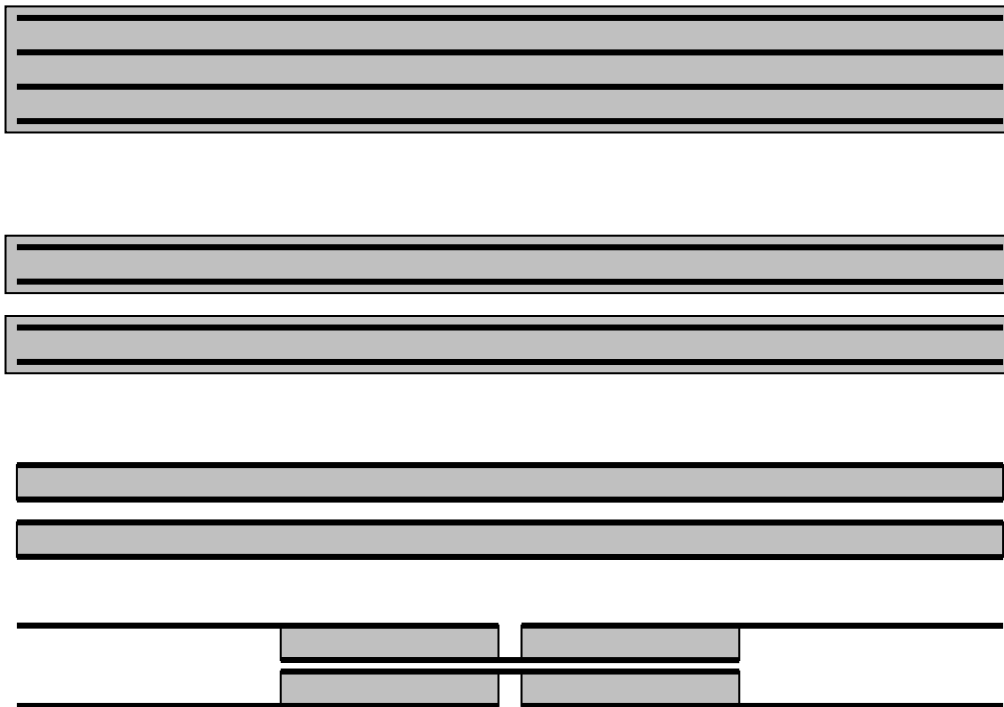


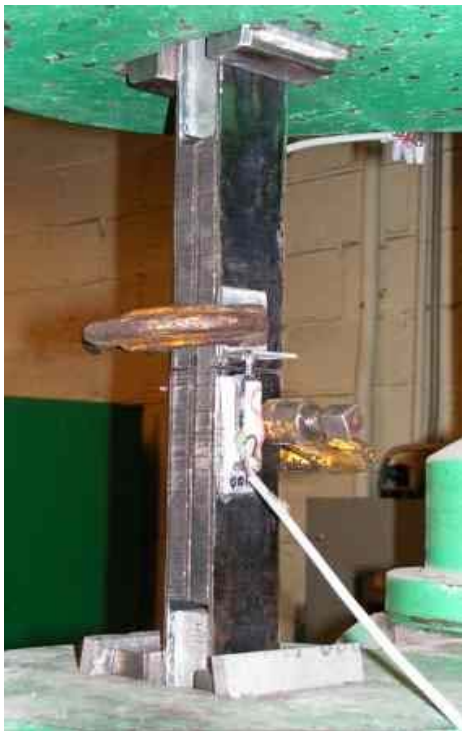
**Figure C-17 Steps in Preparation of Shear Modulus Test Specimens.**

These two pieces are then placed next to each other, and aluminum filler blocks are hot glued between them, so that the ends of the combined specimen can be gripped by the wedge grips of the test machine. The entire specimen is placed into the 120-kip Baldwin Universal Test Machine, which is then loaded slightly to ensure that the test specimen will remain in place. Potentiometers are attached so as to bridge the cuts in the steel plates. As the specimen is stretched, the gap between the two shearing pieces of rubber is measured. The two potentiometers and the test machine load readout are connected to the same HP 4397A data acquisition system as was used in the axial load tests, and testing proceeds





Figure C-18 Shear test specimen in various stages of production. The knife for peeling off rubber is also shown far right.



(a) Unloaded



(b) Loaded

Figure C-19 Shear Modulus Test

The test procedure used here differed slightly from the one prescribed by ASTM D-4014 because the test machine had wedge-grips rather than a bolted attachment system. With a wedge-grip system, the load cannot be reduced to zero without the wedge grips loosening

and the specimen falling out. Therefore the low load (“ $F_I$ ” in ASTM D-4014) could not be as low as specified. If the load-deflection relationship were exactly linear, this would make no difference. However, the curve typically softens slightly in the initial stages, so deriving the secant modulus from a range that is higher up the curve affects the calculated value of the modulus. Furthermore, the first tests were conducted on 5” long specimens, and, through a mis-reading of the specification, they were loaded during the five pre-conditioning cycles to a peak of approximately 100% shear strain, rather than the 50% shear strain implied by ASTM D-4014. During those tests on 5” long specimens, a minimum load,  $F_I$ , was also established, and was used unchanged throughout the subsequent tests on the specimens after they had been cut down in size, even though this caused a shear stress and strain at minimum load that varied according to the specimen size.

These issues are discussed in greater detail in Appendix D.

## **C.6 Bulk Modulus Test**

The Bulk Modulus test is not a part of the suite of quality control tests required by the AASHTO Specifications of bearings, so it is seldom conducted. However, it is needed as input for the Finite Element analyses, because it defines numerically the compressibility of the rubber. Rubber is very nearly incompressible and has to be analyzed by special methods, for which an important parameter is the (small) degree of compressibility that does exist. The goal of the test is to determine the hydrostatic stress required to cause a unit change in volume in the rubber. In the test, a small rubber sample is enclosed within a thick-walled cylinder, and high pressure is applied by a closely-fitting piston. The pressure is measured by the force on the piston. The volume change is measured by the piston displacement.

The unstressed rubber sample should fit the cylinder as closely as possible. If it does not, the load-deflection curve will have a long, soft, lead-in segment, which makes interpretation of the results more difficult. Here, the samples were cut from finished bearings and consisted of alternate layers of steel and rubber.

To prepare the sample specimen of rubber for each batch, a hole-saw is used to cut a 1.5-inch diameter core out of a bearing. As the hole saw cuts deeper into the bearing, side friction increases dramatically and the hole-saw will easily become jammed. To minimize friction, lubricating fluid is poured into the cut periodically, as well as cutting oil for the steel layers. Liberal use of these fluids can keep the bearing temperature below 140 deg F. and prevent significant change of the rubber properties. Typical hole-saws are not deep enough to cut completely through a 2.25-inch thick bearing, so the hole must be cut partly from each side, which requires accurate alignment of the two holes. This is achieved with a metal template, into which a hole is first cut using the same hole-saw. The template is then placed on top of the bearing and three small locating holes are drilled through the template and bearing. The bearing is then turned over, the template is aligned with the location holes, and the hole-saw is used to cut the desired hole.



**Figure C-20 Bulk Modulus Test Rig and Sample**

The test rig for the bulk modulus test consists of a 1.5” diameter steel piston that fits tightly into a steel cylinder with an outer diameter of approximately 3.0”. The specimen is placed in the cylinder and the piston is placed on top of it. The piston has a very tight fit with the inside wall of the cylinder to ensure that rubber does not flow into the gap between the two. The rig is then compressed in the laboratory’s 120-kip Baldwin Test Machine as two potentiometers measure the piston displacement. The piston is compressed five times and returned to nearly its starting point while the potentiometers and the force are recorded once every second by the HP data acquisition system.

Because the samples contained both steel and rubber layers it was necessary to account, in the calculations of bulk modulus, for both the compressibility of the steel layers and the expansion of the surrounding cylinder. Both effects proved to be small compared with the bulk compliance of the rubber, but they were addressed nonetheless.

